09

# Experimental-calculated estimation of fiber laser's response to pulsed X-rays

© S.M. Dubrovskikh, O.V. Tkachev, V.P. Shukailo, A.N. Slobozhanin, A.N. Afanasiev

Russian Federal Nuclear Center — VNIITF, (Federal State Unitary Enterprise „Russian Federal Nuclear Center — Zababakhin All-Russia Research Institute of technical Physics")
456770 Snezhinsk, Chelyabinsk region, Russia
e-mail: S.M.Dubrovskikh@vniitf.ru

*Received March 3, 2023*
*Revised June 1, 2023*
*Accepted July 7, 2023*

Experiments have been carried out to study the transient radiation-induced absorption in the active core of a double-clad ytterbium fiber and the response of a laser based on it under the exposure of pulsed X-rays. It has been found that the time of loss of laser performance (downtime) under pulsed irradiation increases with an increase in the absorbed of radiation and a decrease in the laser pump power and reaches values of $\sim 1$ ms. An analysis of the experimental results shows that the laser response to the X-rays pulse exposure is determined by radiation-induced losses in the active fiber core. An experimental-calculated method for estimating the radiation reaction of a laser, based on the results of studies of the active fiber, is proposed.

**Keywords:** X-rays, fiber laser, radiation-induced attenuation, downtime.

DOI: 10.61011/TP.2023.09.57367.35-23

## Introduction

Today, there is an active development of diode-pumped fiber lasers. High efficiency and quality of laser radiation, small size and mass characteristics make this type of lasers preferable for application in specialized areas of technology: spacecraft, nuclear power systems etc. Applications in these areas require information on hardness to ionising radiation (IR).

From the point of view of analyzing the impact of IR on laser systems, a diode-pumped fiber laser can be represented as three main components: a power supply and control system (radio-electronic equipment, (REE)); a pumping system (laser diodes); and a resonant cavity including an active medium and fiber Bragg gratings (FBGs). The task of ensuring the required level of radiation hardness of REE is traditional and is not an unsolvable problem. As for the pumping system, when modern laser diodes are irradiated with pulsed X-rays or electron radiation, no drop in output power is observed — on the contrary, radiation-induced laser generation [1,2] occurs at the moment of exposure. At the present moment the greatest difficulty is the estimation of sensitivity to IR of optical elements of the laser. This is due to the strong dependence of radiation characteristics on production technology, composition, experimental conditions, etc. [3,4], which makes it difficult to use literature data. It is also necessary to emphasize that the data presented in the published sources, as a rule, concern the effects associated with the accumulated dose of ionising radiation and practically do not consider the effects of pulse exposure of IR.

An analysis of work on dose effects in active fibers, e.g. [5], and Bragg lattices, e.g., [6,7], suggests that the active fiber is the most IR-affected laser element. Literature data [5], as well as experiments conducted by the authors with ytterbium fibers at $Co^{60}$ gamma sources, indicate that significant changes in the characteristics of the active fiber during the accumulation of the IR dose are associated with the growth of non-selective losses of the active core in the range of operating wavelengths 1050–1100 nm.

As for the studies of reversible radiation effects, there are single papers on erbium fibers [8] and no papers on the effects in fiber lasers. Thus, the purpose of the present work was to determine the response of ytterbium fiber laser in different modes of operation to pulsed IR under variation of exposure level and to consider the possibility of its computational-experimental evaluation.

## 1. Experiment procedure

### 1.1. Samples

In the present work, a fiber laser based on an active double-clad aluminosilicate fiber doped with ytterbium ions ($Yb^{3+}$) was investigated. The length of the active fiber was 4 m. The laser resonant cavity was arranged using two FBGs with reflectances > 99 and 5%. A specialized pump laser diode unit was used as a continuous pump radiation source with a wavelength of 975 nm. The watt-ampere characteristic (WAC) of the investigated fiber laser is presented in Fig. 1. The wavelength of the output radiation was 1082 nm.

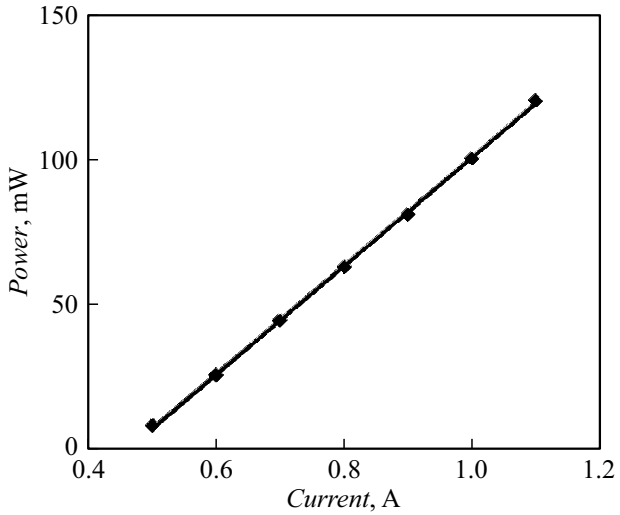


**Figure 1.** WAC of the fiber laser.

The laser was operated in the spike mode [9]. The duration and period of the peaks were regular and were 10 and 25 $\mu$s, respectively (see further, Fig. 3).

Additionally, in the present work, the active fiber from the same batch, on the basis of which the laser was manufactured, was investigated separately. The length of the fiber was 4 m.

### 1.2. Ionising radiation sourse. Dosimetry

The source of pulsed ionising radiation was an electron accelerator generating X-ray pulses with a duration of $\sim$ 30 ns, the average photon energy was $\sim$ 1 MeV.

The X-ray pulse shape was monitored using a semiconductor detector [10]. With the help of thermo-luminescent detectors at the sample location, the exposure dose was monitored with an error of no more than $\pm$20% at each accelerator startup. In this case, according to the calculated estimates, the absorbed dose of IR in the fiber material ($SiO_2$) within the error limits is numerically equal to the exposure dose registered by the detectors.

### 1.3. Measuring techniques

During irradiation of the fiber laser, the relative change in its output power was monitored, the measurement scheme is shown in Fig. 2. Only the optical part of the laser was irradiated, and the exposure level on the FBGs was reduced by two orders of magnitude compared to the one on the active fiber due to the geometry of the experiment.

In experiments were varied IR exposure power and the laser pumping power, which is proportional to the pumping current of the laser diodes.

In the study of the active fiber separately, the relative change in light transmission of the active fiber core during and immediately after the exposure pulse was monitored. Studies were carried out at three wavelengths: 1.08, 1.31 and 1.55 $\mu$m. During the experiments, the irradiated active fiber was coiled into a coil with a diameter of 5 cm and placed directly under the accelerator anode. A fiber laser with wavelength 1.08 $\mu$m was used as a source of scanning radiation with wavelength $\approx$ 100 mW, with wavelengths of 1.31 and 1.55 $\mu$m — optical tester (power $\approx$ 1 mW). The transport of radiation from the testing source to the investigated fiber and from it to the photodetector was carried out yb transport fiber. A reverse biased photodiode with a bandwidth of 200 MHz was used as a photodetector. The magnitude of radiation induced absorption (RIA) was determined, based on Bouguer's law, by the expression

$$\Delta\alpha = \frac{1}{L}\ln\left(\frac{P_{out}^{unirradiated}}{P_{out}^{irradiated}}\right), \qquad (1)$$

where L — length of the irradiated fiber section; $P_{out}^{unirradiated}$, $P_{out}^{irradiated}$ — optical radiation power at the fiber output before and after irradiation.

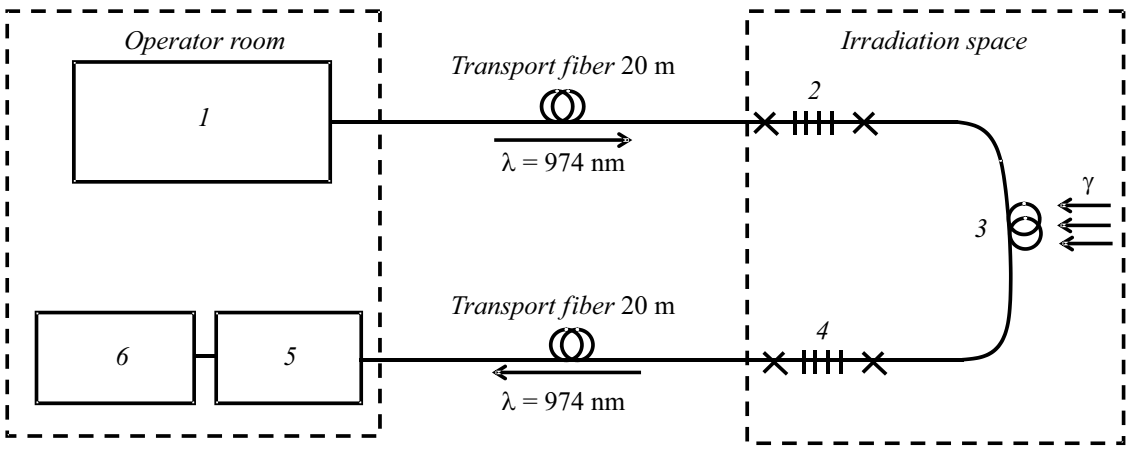


**Figure 2.** Schematic of the experiment to study the effect of pulsed radiation irradiation on the output power of a fiber laser: *1* — laser pump diode unit; *2* — „blind" FBG; *3* — active fiber; *4* — translucent FBG (5%); *5* — photodiode; *6* — digital oscilloscope.

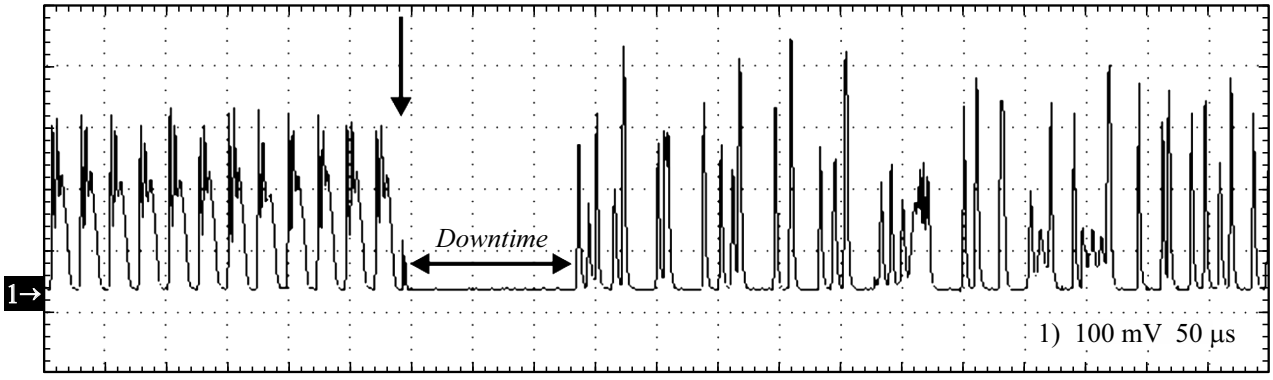


**Figure 3.** Response of a fiber laser exposed to X-ray $D_{imp} \approx 250$ Gy, $I = 1$ A, time sweep 50 $\mu$s/div.

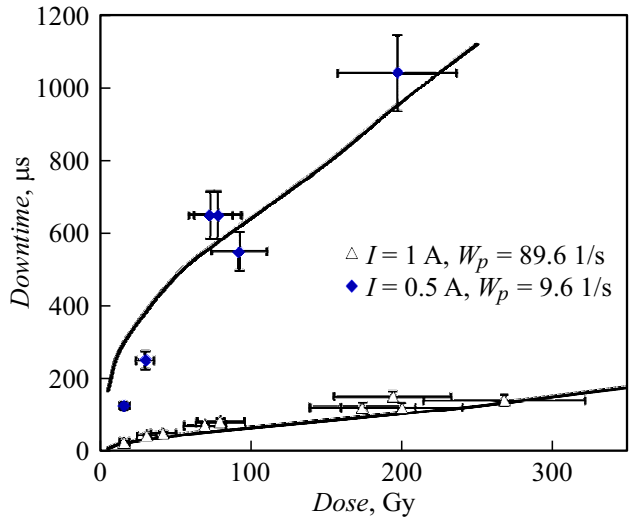


**Figure 4.** Relations of the downtime of a fiber laser on the exposure dose in a pulse: points — experiment, line — calculated estimate.

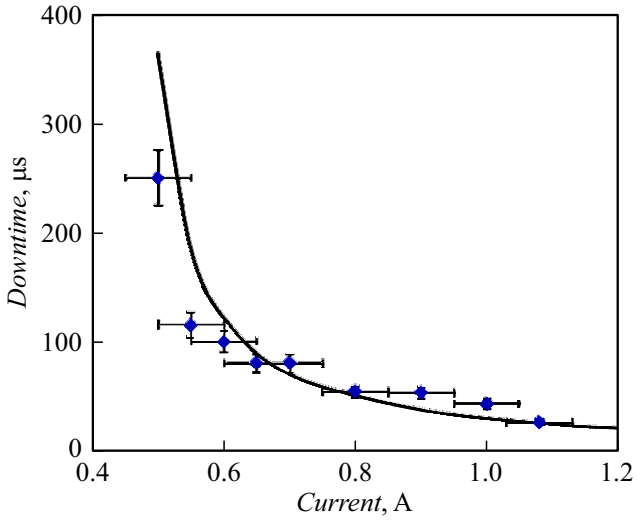


**Figure 5.** Dependence of the downtime of a fiber laser on pump current, $D_{imp} \approx 25$ Gy: points — experiment, line — calculated estimate.

## 2. Experimental results

### 2.1. Effect of a X-ray pulse on the fiber laser operation

Fig. 3 shows the characteristic response of a fiber laser exposed to X-ray pulses at nominal laser operation mode (current of laser pump diodes was $I = 1$exposed to X-ray pulses A) and maximum exposure level (exposure dose in the pulse $D_{imp} \approx 250$ Gy). The arrow in Fig. 3 and in the following oscillograms denotes the moment of exposure to the IR pulse.

From the oscillogram shown in Fig. 3 it can be seen that after pulsed X-ray exposure laser generation breaks off then, after 150 $\mu$s, reduction of laser performance is observed, while the shape of output pulses and frequency change. Measurements one minute after exposure showed that the shape of the output pulses was restored. From the obtained oscillograms we determined the laser loss of performance time (downtime) as the time interval during which generation was absent (Fig. 3). The processing results showed that the downtime relations on the magnitude of the exposure dose in the pulse and the pumping power. Fig. 4 shows the dependences of the laser downtime on the dose in the pulse obtained at the laser operating mode close to threshold ($I = 0.5$ A) and nominal mode ($I = 1$ A). The experimental relations in the investigated range have a logarithmic character. The no-failure rate of the laser, regardless of the mode of operation, is approximately 10 Gy per pulse ($3 \cdot 10^8$ Gy/s).

As can be seen from the relations shown in Fig. 4, the laser downtime depends significantly on the pump current of the laser diodes: at 0.5 to 1 A increase in the current consumption, the laser downtime decreases by about an order of magnitude. The relation of the laser downtime on the pump current at a constant dose in the $D_{imp} \approx 25$ Gy pulse is presented in Fig. 5.

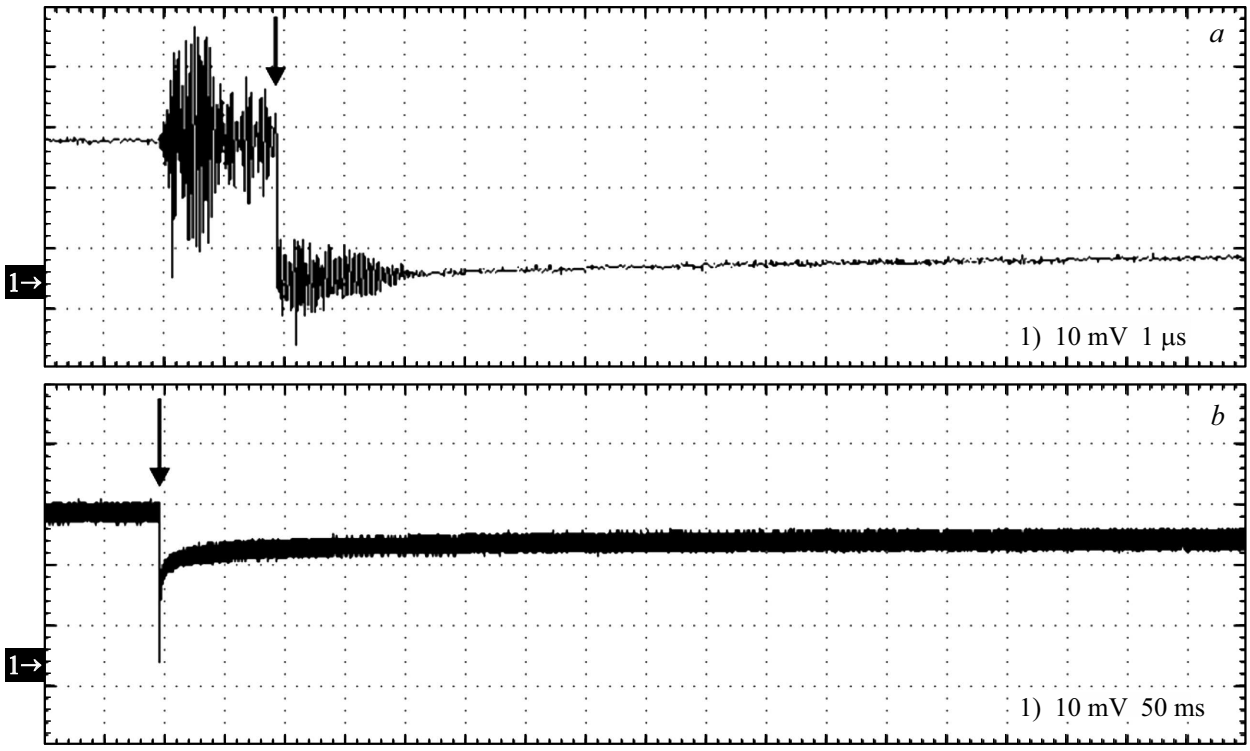


**Figure 6.** Decrease in light transmission of the active fiber core at the time of exposure to the X-ray pulse at different observation interval durations, $D_{imp} \approx 250$ Gy: *a* — temporal sweep 1 $\mu$s/div, *b* — temporal sweep 50 ms/div.

### 2.2. Radiation-induced absorption in active fiber core under pulse exposure

Experiments have shown that in the active fiber core the fiber, the magnitude of optical loss and light transmission relaxation time (up to seconds) do not differ within the measurement error when the scanning radiation wavelength (1.08, 1.31 and 1.55 $\mu$m) and optical signal power (1 and 100 mW) are varied.

Fig. 6 illustrates oscillograms of light transmission decrease of the active fiber core at the moment of exposure pulsed X-ray with duration 25 ns and dose in the pulse $\approx$ 250 Gy.

It can be seen from Fig. 6 that at the moment of exposure, the core of the fiber completely loses its bandwidth. After the exposure pulse, a partial reduction of fiber capacity is observed, with the duration of relaxation processes being much longer than the duration of the exposure pulse. The interference observed on the signal „1“ 2 $\mu$s before and during 2 $\mu$s after the exposure pulse (Fig.6, *a*) is caused by the associated electromagnetic radiation from the electron accelerator induced on the exposed parts of the photodetector, communication lines, and oscilloscope input paths located in the operator room. According to the results of oscillogram processing, the relations of the relative light transmission of the fiber core on the exposure dose were plotted directly at the moment of exposure to the IR pulse and in 0.2 s afterwards (Fig. 7).

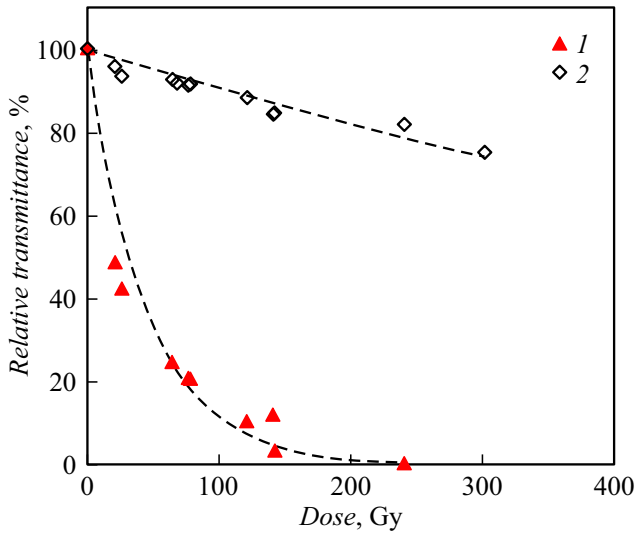


**Figure 7.** Relations of the relative transmission coefficient of the fiber core on the exposure dose in the pulse: *1* — immediately at the moment of exposure to the IR pulse; *2* — after 0.2 s after exposure.

It can be seen from Fig. 7 that at a pulse dose of more than 200 Gy at the moment of exposure, the fiber core completely loses its bandwidth. Within 0.2 s after exposure pulse the value of the relative transmittance is substantially restored.

When the relative transmittance of the fiber core is monitored over long times (minutes), there is a difference in the rate of light transmission relaxation when the irradiation power is changed. At a power of $\sim 100$ mW, the relaxation rate is two times higher than at a power of $\sim 1$ mW. Apparently, this difference is due to the photobleatching, that is annealing of the coloring centers created by ionising radiation, which manifests itself more strongly at higher power of the scanning source. This effect is observed in some irradiated laser crystals and fibers [11,12].

## 3. Analysis of the experiment results

### 3.1. Balance equations of the laser system with accounting for radiation effects

To analyze the data of the fiber laser pulsed irradiation response we consider a system of balance equations for a quasi-two-level system describing the population density of working levels and the photon density in the resonant cavity [13]. The application of the quasi-two-level approximation to ytterbium active media is standard [14], and the transition to it is consistently proved in work [15].

$$\begin{cases} \dfrac{dN_2}{dt} = W_p(N_t - N_2) - \dfrac{N_2}{\tau} - N_2\sigma c\Phi, \\ \dfrac{d\Phi}{dt} = N_2\sigma c\Phi - \dfrac{\Phi}{\tau_{rez}}. \end{cases} \tag{2}$$

Here, $N_2$ — the working level population, [$m^{-3}$]; $N_t$ — $Yb^{3+}$-ion concentration, $N_t \approx 5 \cdot 10^{25}\,m^{-3}$ [14,16]; $W_p$ — pumping speed, [$s^{-1}$]; $\Phi$ — photons concentrations in the resonant cavity, [$m^{-3}$]; $\tau$ — lifetime of the working laser level, $\tau \approx 0.8$ ms [14,16]; $c$ — the light speed in the active medium, [m/s]; $\sigma$ — the forced transition cross section, $\sigma \approx 2 \cdot 10^{-23}\,m^2$ [14,16]; $\tau_{rez}$ — photon lifetime in resonant cavity, [s].

In (2), the first equation describes the change in the population of the working level due to the processes of spontaneous and stimulated emission. The second equation of the system describes the change in photon concentration in the resonant cavity: the first term of the equation accounts for the change in photon concentration due to stimulated emission, while the second term describes the losses in the resonant cavity.

The lifetime of a photon in a resonant cavity, according to [9]:

$$\frac{1}{\tau_{rez}} = \frac{1}{\tau_1} + \frac{1}{\tau_2} = c\alpha_1 + c\alpha_2, \tag{3}$$

where the first term is related to losses on the resonant cavity mirrors (in our case on FBGs), the second term, in the most general case, — with losses in the active medium. We estimate the magnitude of the FBGs loss [9]

$$\alpha_1 = \frac{1}{2L}\ln\left(\frac{1}{R_1R_2}\right),$$

where $L$ — the length of the resonant cavity, $L = 4$ m; $R_1 = 0.99$ and $R_2 = 0.05$ —- the reflectances of „blind" and „semi-transparent" Bragg gratings, respectively, then $\alpha_1 \approx 0.38\,m^{-1}$. The second term of expression (3) is responsible for the losses associated with the absorption of laser radiation by the active medium at the generation wavelength. As shown by measurements of the active fiber characteristics before irradiation, this coefficient for the core of the fiber is $\approx 0.01\,m^{-1}$. Since $\alpha_1 \gg \alpha_2$, then $\alpha_2$ can be neglected in further consideration.

Thus, the parameter $W_p$ remains undetermined. In our case, it is constant in time and equals

$$W_p = k(I - I_{th}), \tag{4}$$

where $I$ — pumping current, [A]; $I_{th}$ — threshold current, $I_{th} = 0.44$ A; $k$ [$(A \cdot s)^{-1}$] — pumping efficiency factor.

To determine the unknown coefficient $k$, consider the expression for the output power of the laser radiation [13]:

$$P = S(I - R_2)h\nu c\Phi, \tag{5}$$

where $S$ — the cross-sectional area of the output beam, [$m^2$], calculated from the characteristic mode diameter of the fiber used ($\approx 8\,\mu$m); $h\nu$ — the photon energy of the output radiation, [J].

In (5), the photon concentration in the resonant cavity $\Phi$ is obtained from solving the system of equations (2) for the stationary case (at $t \to \infty$):

$$\Phi = \frac{W_p\tau\,(N_t\sigma/\alpha_1 - 1) - 1}{\sigma c\tau}. \tag{6}$$

Combining expressions (4) – (6), for the output power we have

$$P = S(1 - R_2)h\nu c\,\frac{\tau\,(N_t\sigma/\alpha_1 - 1) - 1}{\sigma c\tau}\,k(I - I_{th}). \tag{7}$$

The expression (7), which has the form $|P = \text{const}\,k(I - I_{th})$, is an approximating expression for the WAC. The experimental WAC of the fiber laser (Fig. 1) is satisfactorily described by expression (7) at the value of $k = 160\,(A \cdot s)^{-1}$.

As shown in the experimental section, the losses associated with the absorption of laser radiation by the active medium at the generation wavelength increase under radiation exposure, which is due to the formation of coloring centers in the fiber core under the IR influence, which absorb the laser generation radiation. The effect of radiation exposure in the system of equations (2) is logically accounted for by the growth of losses in the active core of the fiber: $\frac{1}{\tau_{rez}} = c\alpha_1 + c\Delta\alpha$, where $\Delta\alpha$ — the coefficient of radiation induced losses in the active fiber core at the generation wavelength, [$m^{-1}$].

Then, we can transform the system of equations (2) to species:

$$\begin{cases} \dfrac{dN_2}{dt} = W_p(N_t - N_2) - \dfrac{N_2}{\tau} - N_2\sigma c\Phi, \\ \dfrac{d\Phi}{dt} = N_2\sigma c\Phi - c\Phi(\alpha_1 + \Delta\alpha). \end{cases} \tag{8}$$

To solve the system of equations (8), it is necessary to know the magnitude of radiation induced losses $\Delta\alpha$.

### 3.2. Radiation induced losses in the core of the active fiber

In Fig. 8, data from oscillograms obtained at pulse dose 120 and 250 Gy (Fig. 6) are plotted in a single graph, where the change in relative transmittance is converted by the expression (1) to radiation-induced absorption.

Experimental data on RIA relaxation in the fiber core were approximated by a set of exponentials:

$$\Delta\alpha = D_{imp}\left(\sum_{i=1}^{7} A_i e^{-t/\tau_i}\right), \qquad (9)$$

where $D_{imp}$ — absorbed dose in the fiber material per pulse, [Gy]; $\tau_i$ — relaxation time constant, [s]. The normalization coefficients $A_i$ in expression (9) were selected taking into account the experimental dependence of the RIA in the core of the active fiber on the dose in the pulse, obtained directly at the moment of the exposure pulse (Fig. 9). The RIA dose dependence (Fig. 9) was obtained by transforming by formula (1) the data presented in Fig. 7.

The normalization coefficients and time constants at which expression (9) satisfactorily approximates the experimental data (Fig. 8) are given in table below.

Thus, expression (9) allows us to describe the relaxation of the RIA in the core of the active fiber in the time range from 0.1 $\mu$s to 1 s after the exposure pulse at different IR dose in the pulse. The impossibility to describe the kinetics of RIA relaxation in the fiber core by a single exponent indicates about large number of types of unstable radiation coloring centers with different lifetimes.

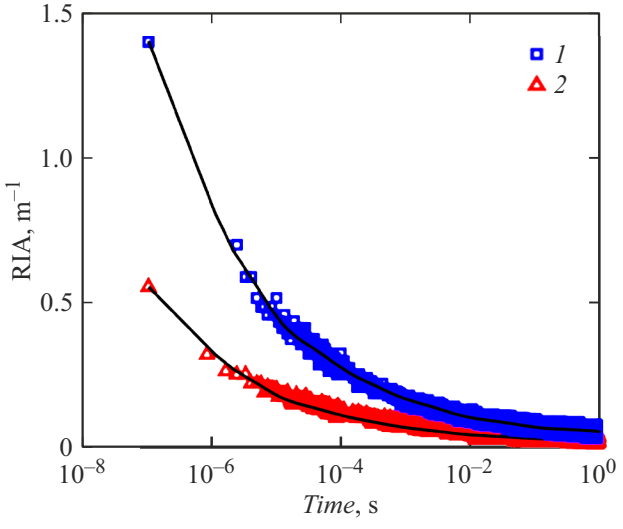


**Figure 8.** Relaxation of RIA in the core of the active fiber after a pulse of IR: *1* — 250 Gy; *2* — 120 Gy.

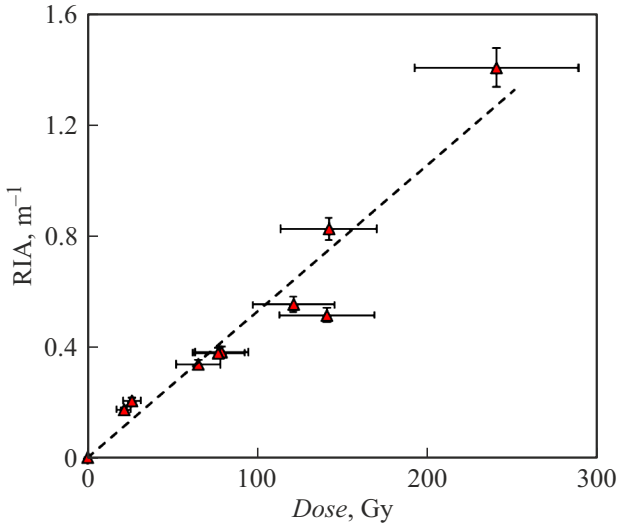


**Figure 9.** Dependence of the RIA value in the core of the active fiber immediately at the moment of exposure on the dose in the pulse.

### 3.3. Simulation results of the laser downtime at IR pulse exposure

The solution of the system of equations (8) taking into account the RIA in the core of the active fiber (9) allows us to simulate the laser response to a pulse X-ray exposure at different radiation load and laser operating mode. The final form of the system of equations by which the photon density in the resonant cavity was calculated:

$$\begin{cases} \dfrac{dN_2}{dt} = k(I - I_{th})(N_t - N_2) - \dfrac{N_2}{\tau} - N_2\sigma c\Phi, \\ \dfrac{d\Phi}{dt} = N_2\sigma c\Phi - c\Phi\left(\dfrac{1}{2L}\ln\left(\dfrac{1}{R_1R_2}\right)\right. \\ \qquad \left. + D_{imp}\left(\sum_{i=1}^{7} A_i e^{-t/\tau_i}\right)\right). \end{cases} \qquad (10)$$

In solving the system of equations (10), the X-ray pulsed exposure was introduced at time $t = 1$ ms. The growth of RIA during the time of radiation exposure was not taken into account: it was assumed that radiation-induced losses occur instantaneously and gradually relax over time. This simplification is quite acceptable since the duration of the X-ray pulse was $\sim 30$ ns, which is a delta pulse with respect to the RIA relaxation time constants (see Table).

An example of calculating the laser response to an exposure pulse at a pulse dose $D_{imp} = 250$ Gy and pump current $I = 1$ A is shown in Fig. 10.

It should be noted that the system of equations (10) is applicable in the case of single-mode generation and does not allow describing the spike mode of laser generation caused by interference of several modes, which takes place in the real case (Fig. 3). However, under the assumption that the RIA in the fiber core are the same for different laser

Norming coefficients and time constants of the approximation of the relaxation RIA relaxation in the core of the active fiber after exposure to a IR pulse

| $i$ | 1 | 2 | 3 | 4 | 5 | 6 | 7 |
|---|---|---|---|---|---|---|---|
| $A_i$, $(\text{Gy}\cdot\text{m})^{-1}$ | $2.8\cdot10^{-3}$ | $1.4\cdot10^{-3}$ | $5.5\cdot10^{-4}$ | $3.8\cdot10^{-4}$ | $2.8\cdot10^{-4}$ | $1.5\cdot10^{-4}$ | $2.3\cdot10^{-4}$ |
| $\tau_i$, s | $5\cdot10^{-7}$ | $5\cdot10^{-6}$ | $5\cdot10^{-5}$ | $3.5\cdot10^{-4}$ | $3.5\cdot10^{-3}$ | $5\cdot10^{-2}$ | 5 |

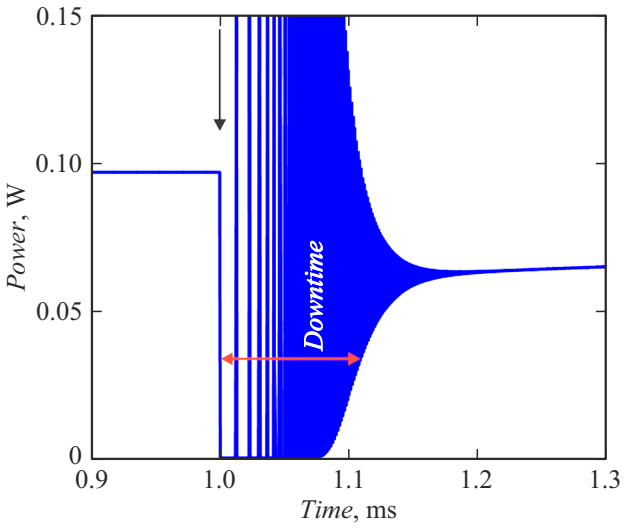


**Figure 10.** Example of calculating the laser response to a stimulus pulse, $I = 1\,\text{A}$, $D_{imp} = 250\,\text{Gy}$.

modes, the solution of the system (10) allows us to estimate the laser recovery time after pulsed exposure to ionising radiation. As can be seen from the simulation results, a breakdown of laser radiation generation is observed at the moment of exposure, and then a gradual emergence to the stationary mode. Reduction of continuous output power to 50% of the initial value was considered to be the criterion for restoring laser performance. Solution of the system of equations (10) at various exposure levels ($D_{imp}$) allows us to obtain the calculated dependence of the downtime on the exposure dose in the pulse. On Fig. 4 together with the experimental data the calculated dependences of the laser downtime on the dose in the pulse at the nominal mode of laser operation ($I = 1\,\text{A}$, $W_p = 89.6\,\text{s}^{-1}$) and at threshold ($I = 0.5\,\text{A}$, $W_p = 9.6\,\text{s}^{-1}$) are presented. Fig. 5 shows experimental data and calculated dependence of the downtime of the laser on the pump current. The good agreement of the calculation results with experimental data indicates the correctness of the assumption that the response of a fiber laser under pulsed X-ray exposure of its optical part is determined by RIA in the active core of the fiber at the generation wavelength. By increasing the pump power, the laser downtime can be significantly reduced after exposure to the IR pulse. The approach considered in the present work allows one to estimate, from experimental RIA data in the core of the active fiber at the generation wavelength, the downtime of a fiber laser at different levels of radiation exposure and laser operation mode.

## Conclusion

Experiments have been carried out to investigate the response of a fiber laser when a X-ray pulse exposed to its optical part. It has been obtained that the time of laser performance loss under pulse irradiation increases with the increase of the exposure dose rate IR and decrease of the laser pumping power and reaches the values $\sim 1$ ms. The analysis of experimental results shows that the laser response is determined by RIA in the active core of the fiber. The approach considered in this work allows, according to experimental data, specifically RIA in the active fiber core at the generation wavelength and WAC of the laser to estimate the downtime of the fiber laser at different level of ionizing radiation exposure and laser system pump power.

### Acknowledgments

The authors are grateful to A.S. Pilipenko and M.G. Slobozhanina for valuable comments.

### Conflict of interest

The authors declare that they have no conflict of interest.

## References

[1] N.V. Basargina, I.V. Vorozhtsova, S.M. Dubrovskikh, E.V. Smirnov, O.V. Tkachev, A.V. Fomin, V.P. Shukailo. VANT series: Fizika radiatsionnogo vozdeystviya na radioelektronnuyu apparaturu, **4**, 35 2013 (in Russian).
[2] M.M. Zverev, N.A. Gamov, E.V. Zhdanova, D.V. Peregudov, V.B. Studionov, M.A. Ladugin, A.A. Marmaluk. Opt. Spectr., **111** (2), 182 (2011). DOI: 10.1134/S0030400X11080339
[3] P.F. Kashaykin. Kand. diss. (NTsVO RAN, M., 2019)
[4] K.V. Zotov. Avtoref. kand. diss. (NTsVO RAN, M., 2010)
[5] S. Girard, Y. Ouerdane, B. Tortech, C. Marcandella, T. Robin, B. Cadier, J. Baggio, P. Paillet, V. Ferlet-Cavrois, A. Boukenter, J.-P. Meunier, J.R. Schwank, M.R. Shaneyfelt, P.E. Dodd, E.W. Blackmore. IEEE Trans. Nucl. Sci., **56** (6), 3293 (2009). DOI: 10.1109/TNS.2009.2033999
[6] A.I. Gusarov, S.K. Hoeffgen. IEEE Trans. Nucl. Sci., **60** (3), 2037 (2013). DOI: 10.1109/TNS.2013.2252366

[7] A.V. Faustov, A.I. Gusarov, P. Mégret, M. Wuilpart, D. Kinet, A.A. Fotiadi, A.V. Zhukov, S.G. Novikov, V.V. Svetukhin. Quant. Electron., **46** (2), 150 (2016). DOI: 10.1070/QEL15879
[8] A.A. Ponosova, I.S. Azanova, O.L. Kel, Y.O. Sharonova, N.K. Mironov, M.V. Yashkov, K.E. Riumkin, M.A. Melkumov. Quant. Electron., **49** (7), 693 (2019). DOI: 10.1070/QEL16833
[9] O. Zvelto. Printsipy lazerov (SPb., Lan', 2008) (in Russian).
[10] V.V. Vorobyev, V.N. Afanasyev, V.F. Khokhryakov. PTE, **1**, 85 (1974). (in Russian).
[11] V.P. Shukailo, O.V. Tkachev, S.M. Dubrovskikh, T.V. Kupyrina. VANT series: Fizika radiatsionnogo vozdeystviya na radioelektronnuyu apparaturu, **1**, 18 (2020). (in Russian).
[12] E.M. Dianov, L.S. Kornienko, E.P. Nikitin, A.O. Rybaltovsky, V.B. Sulimov, P.V. Chernov. Soviet J. Quant. Electron., **13** (3), 274, (1983). DOI: 10.1070/QE1983v013n03ABEH004145
[13] Y. Aichler, G.I. Aichler. Lasers. *Ispolneniye, upravleniye, primeneniye* (Technosfera, M., 2012)
[14] R. Paschotta, J. Nilsson, A.C. Tropper, D.C. Hanna. IEEE J. Sel. Top. Quant. Electron., **33** (7), 1049 (1997). DOI: 10.1364/OE.21.013818
[15] M.G. Slobozhanina, A.V. Bochkov, A.N. Slobozhanin. Opt. Fib. Technol., **63**, 102512 (2021). DOI: 10.1016/j.yofte.2021.102512
[16] N.M. Pask, R.J. Carman, D.C. Hanna, A.C. Tropper, C.J. Mackechnie, P.R. Barber, J.M. Dawes. IEEE J. Sel. Top. Quant. Electron., **1** (1), 2 (1995). DOI: 10.1109/2944.468377

*Translated by Y.Deineka*